

**PHYSICAL AND MINERALOGY CHARACTERISTICS OF THE LUNAR REGOLITH IN THE AREAS OF THE THERMAL ANOMALIES.** S. G. Pugacheva, V.V. Shevchenko. Sternberg State Astronomical Institute, Moscow University, Russia, [pugach@sai.msu.ru](mailto:pugach@sai.msu.ru)

In the previous papers we considered correlation the Lunar Prospector thorium contents with structure of the lunar surface [1]. The surface roughness was estimated by means comparison of the local phase function and the average integrated lunar indicatrix. The average integrated lunar indicatrix was used as a background photometric model [2]. The great difference between the modelled and observed phase functions for phase angle in range about  $18^\circ$  demonstrates a high degree of the surface roughness. The value of this difference of intensities was used as a photometric parameter of the surface roughness. A good correlation between the local size-frequency distribution of the fragments and photometric parameter of roughness was observed. Comparison of the local cumulative number of the particles (N per  $10^4 \text{ m}^2$ ) and photometric roughness parameter ( $\Delta I$ ) shows in Figure 1.

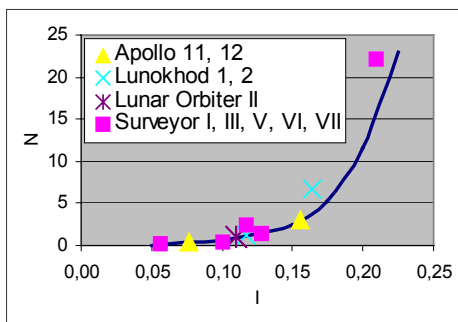


Figure 1. Comparison of the local cumulative number of particles N per  $10^4 \text{ m}^2$  and photometric roughness parameter  $\Delta I$ .

In this report we research data of the IR thermal radiation, the rough structure of the lunar regolith and mineralogy characteristics upper layer of the surface. The analytic model of the lunar thermal field was realized as an angular function of the thermal infrared radiation in the IR spectral region (10-12 micron). The basic material for investigations is the scanned cosmic spectrozonal images of the lunar surface transmitted by the first Russian geostationary artificial meteorological satellite of the Earth "GOMS" [3]. The model the surface described the surface-temperature by the radiation temperature vector in the range of positive values of the angular parameters: the incidence angle ( $i$ ), the reflection angle ( $\epsilon$ ), and the azimuth angle between the plane of the incident and reflected rays ( $A$ ). Figure 2 shows diagram of the vector of the thermal radiation for angle incidence of the solar-light  $i = 60^\circ$ , the reflection angle  $\epsilon = 0^\circ - 90^\circ$ , and the azimuth angle  $A = 0^\circ - 180^\circ$ .

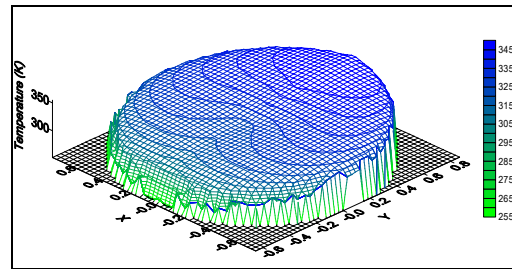


Figure 2. The spatial graphical function of the lunar-surface thermal radiation.

A comparison of the analytic model of the lunar thermal field and radiation temperatures measured shows a systematic departure of the measured values from the average values. The statistical analysis of the photometry database given lunar sites has allowed allocating 4 groups of thermal anomalies. The sites of the surface having a different thermal conduction of the ground, sites located on the edge of the Moon's limb, "hot spots" - sites, which area are less than the sanction of the detector, anomalies stipulated by the relief concern to thermal anomalies. Thermal anomalies connected to relief may be related to non-stationary thermal phenomena. The thermal anomalies are dated for such large craters as Copernicus, Tycho, Stevinus and other craters. That is called by irregularities of the relief of the crater floor. On detail study of large-scale photographs some anomalies are identified with small-sized craters, others with separate clusters of stones. Images of the crater Copernicus and crater Tycho are shown on the figures 3, 4. The difference of the surface temperature these thermal anomalies exceed 20 K, the value of the cumulative number of particles composes 4 and 32 respectively.

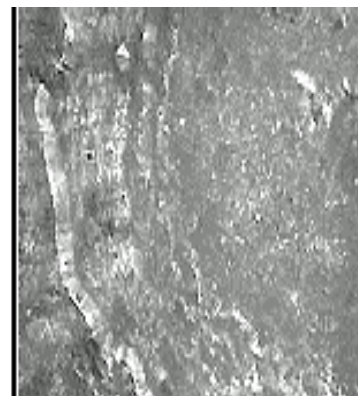


Figure 3. Image of the crater Copernicus (94 km,  $10^\circ\text{N}$ ,  $20^\circ\text{W}$ , Clementine picture).



Figure 4. Image of the crater Tycho (87 km, 43°S, 11°W, Clementine picture)

The values of thorium contents and iron contents for separate sites of the lunar surface have been determined under catalogue Lawrence [4].

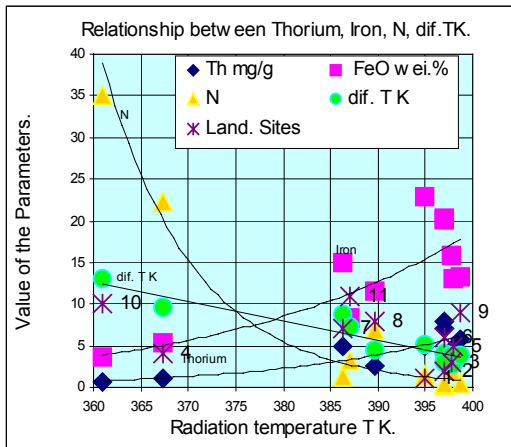


Figure 5. Thorium and iron contents in the landing sites: Surveyor I (43°W, 2°S), Surveyor III (23°W, 3°S), Surveyor V (23°E, 1°N), Surveyor VI (1°W, 0°N), Surveyor VII (11°W, 41°S), Apollo 11 (22°E, 1°N), Apollo 12 (23°W, 3°S), Lunokhod 1 (35°W, 38°N), Lunokhod 2 (30°E, 26°N), Lunar Orbiter II.

We have compared the data of thorium and iron contents and the value IR radiation temperature of the surface for landing sites. It's observed a good correlation between temperature T K and the local Th-content, between temperature T K and FeO-content. The lines of the polynomial trend of the dependence of radiation temperature, thorium content and iron content, quantity of particles, difference of the measure and calculation temperature were shown on diagram (figure 5). The separate points on diagram represent areas of landing sites: Surveyor I (1), Surveyor III (2), Surveyor V (3), Surveyor VII (4), Apollo 11 (5), Apollo 12 (6), Lunokhod 1 (7), Lunokhod 2 (8), Surveyor VI (9). The numbers of landing sites on the diagram (figure 5, "Land. Sites") are indicated in brackets. The number of the crater Tycho on the diagram (figure 5) is 10; the number of the crater Copernicus is 11.

The Saari and Shorthill catalogue data were used as investigation correlation between the local thorium content and the photometry roughness parameter (Figure 6). The correlation coefficient between temperature and local Th-content is 0,89, between temperature and photometry index is -0,75.

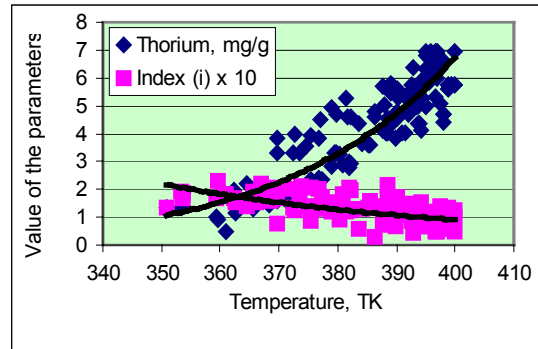


Figure 6. Comparative data of thorium content and photometric roughness parameter for 150 points of the Saari and Shorthill catalogue data [5].

Table gives the parameters of the regression coefficients of the equation ( $Y = a \cdot T + b$ ) for temperature-thorium (T-Th) and temperature-photometric index (T-ΔI), means values (m), correlation coefficients (r), standard deviations ( $\sigma$ ).

Table				
Statistics Data				
	$Y = a \cdot T + b$	m	$\sigma$	r
TK		384,9	10,8	
Th.	$0,12 \cdot T - 41,7$	4,3	1,4	0,89
ΔI	$-0,02 \cdot T + 9,82$	1,2	0,3	-0,75

We may propose that possible KREEP-rich materials and the anomalies of the radiation temperature associated with photometry roughness of the crater floor. Probably, Th and FeO enter into composition of ejecta lunar materials; these are located on the surface or small depth. KREEP-rich materials are concentrated to mare basalt with a high content FeO. The local assimilation KREEP-rich materials ascribed to volcanic extrusions released or localized by impact and essentially influence on thermal balance of the Moon.

**References:**

[1] Pugacheva S.G., Shevchenko V.V. (2003) LPS XXXIV, 1112. [2] Shevchenko V.V. (1980) The modern selenography. "Nauka Press"(In Russian). [3] Pugacheva S.G., Shevchenko V.V. (2001) Astron. Vestn., vol.35, no.3, pp.199-207. [4] Lawrence D.J. et al. (2000) JGR, 105, No. E8, 20,307-20,331. [5] Shorthill R.W. et al. (1969). Nasa CR-1429.